# Choice of Coordination Number in d$^{10}$ Complexes of Group 11 Metals

M. Angels Carvajal,[†] Juan J. Novoa,[†,‡] and Santiago Alvarez*,[†,§]

*Contribution from the Centre Especial de Recerca en Química Teòrica, Parc Científic de Barcelona, Av. Baldiri Reixach 10-12, 08028 Barcelona, Spain; Departament de Química Física, Universitat de Barcelona, Martí i Franqués 1-11, 08028 Barcelona, Spain; and Departament de Química Inorgànica, Universitat de Barcelona, Martí i Franquès 1-11, 08028 Barcelona, Spain*

Received September 9, 2003; E-mail: santiago.alvarez@qi.ub.es

***Abstract:*** The distribution of di-, tri-, and tetracoordination among the d$^{10}$ ions of the group 11 metals is theoretically analyzed by means of density functional calculations on more than 150 model complexes of general formula $[MX_mL_n]^{(1-m)}$ (where M = Cu, Ag, or Au; L = $NH_3$ or $PH_3$; X = Cl, Br, or I; $m + n = 2-4$). The energy of a ligand association reaction has been found to be practically determined by two contributions: the interaction energy and the energy of deformation of the metal coordination sphere. The larger deformation energy of gold complexes compared to copper and silver ones explains the predominance of dicoordination among Au$^I$ complexes, in comparison with Cu$^I$ and Ag$^I$, for which dicoordination is far less common than tri- and tetracoordination. Other experimental trends can be explained by looking at the fine details of these two energetic components.

## Introduction

The d$^{10}$ ions of the group 11 transition metals present variable coordination numbers, offering one of the most challenging cases for the a priori prediction of the structure expected for a given combination of metal ion and ligands. Hence, one can find many dicoordinate linear molecules but also trigonal planar or tetrahedral complexes. In addition, the distribution of these coordination numbers is clearly different for Au than for the lighter elements of the group, as illustrated in Figure 1. Thus, while Cu$^I$ and Ag$^I$ are most commonly found as tetracoordinate species, Au$^I$ appears essentially in linearly dicoordinate complexes, even if the existence of tri- and tetracoordinate species is nonnegligible.[1] Although in the gas phase only structures of mono- and dicoordinate complexes have been reported,[2] recent FT ion cyclotron resonance spectrometry showed that Cu$^I$ reacts with PH$_3$ forming the di-, tri-, and tetracoordinate cations, whereas Ag$^I$ and Au$^I$ only form dicoordinate complexes.[3] Also recent computational studies[4] have found that bonding of additional phosphine ligands to [Au(PH$_3$)$_2$]$^+$ and [MCl(PH$_3$)] is little favored.

A further complication results from the fact that the assignment of a coordination number in a particular crystal structure is not always straightforward, and some ambiguity exists in a number of cases (see Supporting Information for more details, Table S1). As an example, in Ag$^I$ complexes described as
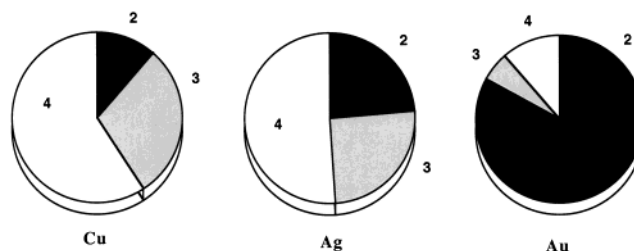


**Figure 1.** Distribution of the crystal structures of Cu$^I$, Ag$^I$, and Au$^I$ compounds according to coordination number of the metal atom as found in the Cambridge Structural Database.

dicoordinate, the L−Ag−L bond angles show a continuous distribution (Supporting Information, Figure S1) between the maximum at 180° and 110°. Deviation from linearity makes us suspect that the smallest bond angles correspond to tricoordinate complexes, as actually found: all molecules with bond angles smaller than 147° are seen to have metal−ligand contacts at less than 2.8 Å, with only one exception.[5] Similarly, many supposedly tricoordinate complexes present either one additional short contact to a donor atom, indicating effective tetracoordination, or one too long "bond distance" that should be considered nonbonding, indicating an effective coordination number of two. Finally, a host of tetracoordinate complexes have either one long metal−ligand bond distance and bond angles consistent with tricoordination or two long bond distances and a nearly linear arrangement of the other two ligands, indicative of effective dicoordination.

With all these precedents, three main questions arise: (1) What determines the coordination number for a given choice of d$^{10}$ metal ion and ligands? (2) Why Au$^I$ has a much greater

[†] Parc Científic de Barcelona.
[‡] Departament de Química Física, Universitat de Barcelona.
[§] Departament de Química Inorgànica, Universitat de Barcelona.

 (1) Gimeno, M. C.; Laguna, A. *Chem. Rev.* **1997**, *97*, 511.
 (2) Vogt, J.; Mez-Starck, B.; Vogt, N.; Hutter, W. *J. Mol. Struct.* **1999**, *485–486*, 249.
 (3) Harris, H.; Fisher, K.; Dance, I. *Inorg. Chem.* **2001**, *40*, 6972.
 (4) Schwerdtfeger, P.; Hermann, H. L.; Schmidbaur, H. *Inorg. Chem.* **2003**, *42*, 1334.
 (5) Kanatzidis, M. G.; Jun-Hong, C. *J. Solid State Chem.* **1996**, *127*, 186.

tendency to appear as di- than as tri- or tetracoordinate complexes, while the opposite seems to happen for Cu$^I$? (3) Why is there such a large degree of ambiguity in the assignment of coordination numbers? In the work reported here, we addressed these questions by performing a theoretical study on a variety of di-, tri-, and tetracoordinate complexes of group 11 transition metals in their +1 oxidation state. The choice of model systems has been designed to represent systematic variations in both metals and ligands, including simplified versions of experimentally known structures. On the selected model systems, we report density funcional calculations carried out to obtain the optimized structures and analyze the thermodynamic tendency of di- or tricoordinate complexes to increase the number of coordinated ligands by looking at the energetics of their ligand association reactions (eqs 1 and 2, where A, B, C, and D represent ligands). Finally, we will discuss the relative importance of different contributions to the formation energies, among which the most relevant ones are the stabilization gained by the formation of a new metal−ligand bond and the destabilization induced by the required deformation of the coordination sphere (e.g., from a linear dicoordinate MAB molecule to a bent fragment at 120°). We have chosen to study the families of compounds of general formula $[MX_mL_n]^{(1-m)}$ (where M = Cu, Ag, or Au; L = $NH_3$ or $PH_3$; X = Cl, Br, or I) because there is a large number of structurally characterized compounds with phosphine, amine, and halide ligands for the three metals in different coordination numbers. Although $NH_3$ and $PH_3$ are rather simplified versions of the amines and phosphines actually found in experimental compounds, it has been shown for the group 11 d$^{10}$ ions that $PH_3$ gives similar results to $PMe_3$, with slightly larger M−P bond lengths and somewhat smaller dissociation energies.[6]

$$[MAB] + C \rightarrow [MABC] \qquad (1)$$

$$[MABC] + D \rightarrow [MABCD] \qquad (2)$$

## Methodology

**Decomposition of the Formation Energies.** The tendency of a given complex to increase its coordination number through ligand association can be computationally represented by comparing the calculated energies before and after metal−ligand bond formation (eqs 1 and 2), by means of the formation energy ($E_f$, defined as the difference between the energies of the products and the reactants in their optimum structures). Thus, to evaluate the stability of a tricoordinate complex relative to that of the dicoordinate one, we compute the formation energy for eq 1. We have found it useful to decompose the formation energy $E_f$ into four contributions, according to eq 3, that corresponds to the thermodynamic cycle shown in Scheme 1.

$$E_f = E_{int} + E_{bend} + E_{str} + E_{pre} \qquad (3)$$

Here, $E_{bend}$ is the energy required to bend the [MAB] dicoordinate complex from its nearly linear optimized structure to the bond angle in the tricoordinate complex, while keeping the bond distances frozen; $E_{str}$ is the energy associated with changes in the M−A and M−B bond distances from the di- to the tricoordinate complex, allowed to relax after bending; $E_{int}$ is the energy of interaction between the dicoordinate [MAB] group and the entering ligand, both with the same geometry that they present in the tricoordinate [MABC] complex; and $E_{pre}$ is the preorganization energy of ligand C from its optimum geometry as a

(6) Bowmaker, G. A.; Schmidbaur, H.; Krüger, S.; Rösch, N. *Inorg. Chem.* **1997**, *36*, 1754.

*Scheme 1*
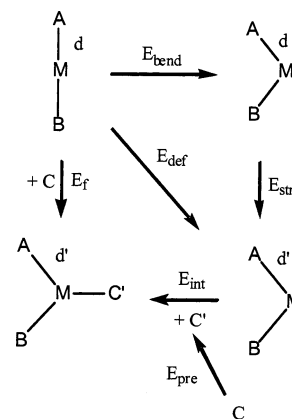


*Scheme 2*
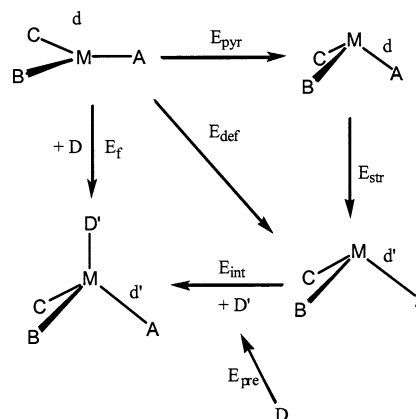


free molecule to its geometry when coordinated to the metal atom in the complex (C′).

Similarly, the formation energy $E_f$ of a tetracoordinate complex through ligand association to a tricoordinate precursor (eq 2) gives us a measure of its tendency to increase its coordination number and can be decomposed into four contributions (Scheme 2).

$$E_f = E_{int} + E_{pyr} + E_{str} + E_{pre} \qquad (4)$$

Now $E_{pyr}$ is the energy required to distort the [MABC] tricoordinate complex from its trigonal planar optimized structure to the pyramidalized fragment in the tetracoordinate complex; $E_{str}$ is the energy associated with changes in the M−A, M−B, and M−C bond distances from the tri- to the tetracoordinate complex; $E_{int}$ is the interaction energy between the tricoordinate precursor and the entering ligand, both with the same geometry that they present in the tetracoordinate product; and $E_{pre}$ is the energy needed to preorganize ligand D from its optimum geometry as a free molecule to that once coordinated to the metal atom (D′).

**Computational Details.** All calculations reported in this work were performed with the GAUSSIAN98 suite of programs[7] using the hybrid B3LYP method.[8] A triple-$\zeta$ basis set used was obtained by decontracting the function with the smallest exponent in the standard LANL2DZ basis set that includes effective core pseudopotentials for the innermost core

(7) Frisch, M. J.; Trucks, G. W.; Schlegel, H. B.; Gill, P. M. W.; Johnson, B. G.; Robb, M. A.; Cheeseman, J. R.; Keith, T. A.; Petersson, G. A.; Montgomery, J. A.; Raghavachari, K.; Al-Laham, M. A.; Zakrzewski, V. G.; Ortiz, J. V.; Foresman, J. B.; Cioslowski, J.; Stefanov, B. B.; Nanayakkara, A.; Challacombe, M.; Peng, C. Y.; Ayala, P. Y.; Chen, W.; Wong, M. W.; Andres, J. L.; Replogle, E. S.; Gomperts, R.; Martin, R. L.; Fox, D. J.; Binkley, J. S.; Defrees, D. J.; Baker, J. P.; Stewart, J. P.; Head-Gordon, M.; Gonzalez, C.; Pople, J. A. *Gaussian 94*, revision E.1; Gaussian, Inc.: Pittsburgh, PA, 1995.
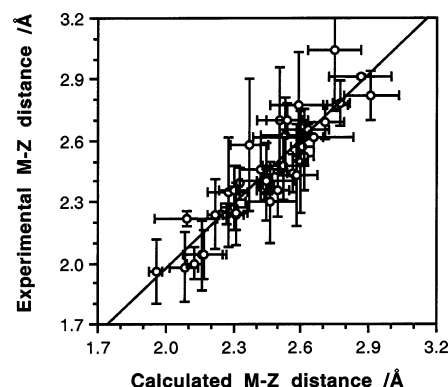(8) Becke, A. D. *J. Chem. Phys.* **1993**, *98*, 5648.

orbitals.[9] Two polarization functions were added per each non-hydrogen atom (of p type for Cu and of d type for Cl and N[10]) as well as diffuse s, p, and d functions (exponents used for the polarization and diffuse functions given as Supporting Information, Table S2). Interaction and dissociation energies were corrected for the basis set superposition error (BSSE) by means of the counterpoise method[11] for several families of reactions $[CuL^1L^2] + L^3$ (Supporting Information, Table S3). Although the BSSE is not negligible, corrected and uncorrected energies give essentially the same trends within a given family of compounds. Only for the $[CuX_2]^- + X^-$ reactions is the dependence of $E_{int}$ on the halide inverted when the results are corrected for the BSSE, but it has been stated that the counterpoise method exaggerates the BSSE correction for the interaction between an anionic complex and an anionic ligand.[12] The influence of the dielectric environment provided by a solvent in solution on the stability of the charged species was studied for the tricoordinate Cu[I] complexes using the nonequilibrium implementation of the polarizable continuum model in its conductor version (CPCM)[13,14] when the medium is water (dielectric constant 78.39) or dichloromethane (8.93). A similar effect should be expected due to the Madelung potential of the counterions in the solid state.

## Results

**Optimized Geometries.** We have calculated the tricoordinate complexes resulting from the following ligand association reactions (L = NH$_3$ or PH$_3$; X = Cl, Br, or I; M = Cu, Ag, or Au),

$$[ML_2]^+ + X^- \rightarrow [MXL_2] \tag{5.1}$$

$$[ML_2]^+ + L \rightarrow [ML_3]^+ \tag{5.2}$$

$$[MXL] + X^- \rightarrow [MX_2L]^- \tag{5.3}$$

$$[MXL] + L \rightarrow [MXL_2] \tag{5.4}$$

$$[MX_2]^- + X^- \rightarrow [MX_3]^{2-} \tag{5.5}$$

$$[MX_2]^- + L \rightarrow [MX_2L]^- \tag{5.6}$$

as well as the tetracoordinate complexes formed in the following ligand association reactions

$$[ML_3]^+ + X^- \rightarrow [MXL_3] \tag{6.1}$$

$$[ML_3]^+ + L \rightarrow [ML_4]^+ \tag{6.2}$$

$$[MXL_2] + X^- \rightarrow [MX_2L_2]^- \tag{6.3}$$

$$[MXL_2] + L \rightarrow [MXL_3] \tag{6.4}$$

$$[MX_2L]^- + X^- \rightarrow [MX_3L]^{2-} \tag{6.5}$$

$$[MX_2L]^- + L \rightarrow [MX_2L_2]^- \tag{6.6}$$

$$[MX_3]^{2-} + X^- \rightarrow [MX_4]^{3-} \tag{6.7}$$

$$[MX_3]^{2-} + L \rightarrow [MX_3L]^{2-} \tag{6.8}$$

(9) Hay, P. J.; Wadt, W. R. *J. Chem. Phys.* **1985**, *82*, 299.
(10) Huzinaga, S.; Andzelm, J.; Klobukowski, M.; Radzi-Andzelm, E.; Sakai, Y.; Tatewaki, H. *Gaussian Basis Sets for Molecular Calculations*; Elsevier: Amsterdam, 1984; polarization functions.
(11) Boys, S. F.; Bernardi, F. *Mol. Phys.* **1970**, *19*, 553.
(12) van Wüllen, C. *J. Chem. Phys.* **1996**, *105*, 5485.
(13) Adamo, C.; Barone, V. *Chem. Phys. Lett.* **2000**, *330*, 152.
(14) Cossi, M.; Barone, V. *J. Phys. Chem. A* **1998**, *102*, 1995.

**Figure 2.** Experimental and calculated M−Z distances for different families of d[10] complexes of the type $[MZL_{n-1}]$, where M = Cu, Ag, or Au; Z is Cl, Br, I, or an N− or P− donor ligand; L is any ligand; and $n = 2-4$. The error bars indicate the ranges of values found within each family. Experimental values for tricoordinate complexes with L−M−L bond angles larger than 150° and tetracoordinate complexes with a sum of the three L−M−L bond angles larger than 350° were disregarded. Experimental structural data have been taken for mononuclear complexes with $R < 10\%$ only.

The most relevant structural data from the optimized geometries of 153 complexes studied (33 di-, 51 tri-, and 69 tetracoordinate), together with the ranges of bond distances and angles found in experimental structures of complexes with the same metal atom and donor set, are deposited as Supporting Information (Tables S4−S8). Of those compounds, 80 were fully optimized (see below). Among the optimized structures, some correspond to distorted geometries due to the formation of intramolecular hydrogen bonds (a problem associated with the use of NH$_3$ and PH$_3$ as simplified model ligands having relatively acid hydrogen atoms), while for a number of complexes geometry optimization led to dissociation of one or two ligands that become attached to the low coordinate complex through intermolecular hydrogen bonding involving the dissociated PH$_3$ or NH$_3$ ligands (these optimized structures are not reported here). Similar results have been found by other researchers in $[Ag(NH_3)_n]^+$ and $[Co(H_2O)_n]^{2+}$ complexes.[15,16] For that reason, we found it adequate in those cases to freeze the bond angles around the metal atom and optimize only the bond distances to avoid the artifactual dissociation. The NH$_3$ and PH$_3$ ligands used in our calculations adequately represent amine and phosphine ligands except for their hydrogen-bonding ability and a slightly less basic character,[17] and comparison of the calculated bond distances with experimental values (Figure 2) shows this to be a sensible approach. To further verify these ideas, we have also optimized a few complexes in which the neutral ligands have methyl rather than hydrogen substituents, namely $[MCl(EMe_3)_2]$ complexes (M = Cu, Ag, or Au and E = N or P, provided as Supporting Information, Table S9). The rest of the complexes that could not be properly optimized were computationally unstable toward ligand dissociation and are thus not expected to appear with the higher coordination number in the gas phase, although we will show below that the dielectric environment (solvent or counterions) may stabilize some of them in condensed phases.

To understand the effect of the chemical composition on the stability of a given complex, we need to compare similar

(15) Fox, B. S.; Beyer, M. K.; Bondybey, V. E. *J. Am. Chem. Soc.* **2002**, *124*, 13613.
(16) Schmiedekamp, A. M.; Ryan, M. D.; Deeth, R. J. *Inorg. Chem.* **2001**, *41*, 5733.
(17) Hancock, R. D.; Martell, A. E. *Comments Inorg. Chem.* **1988**, *6*, 237.

**Table 1.** Calculated Interaction ($E_{int}$) and Formation ($E_f$) Energies (kcal/mol) between Dicoordinate Complexes (at Fixed Bond Angles of 120°) and Neutral (L) or Anionic ($X^-$) Ligands[a]

| | L | $X^-$ | Cu | | Ag | | Au | |
|---|---|---|---|---|---|---|---|---|
| | | | $E_{int}$ | $E_f$ | $E_{int}$ | $E_f$ | $E_{int}$ | $E_f$ |
| $[ML_2]^+ + X^-$ | $NH_3$ | $Cl^-$ | −142.1 | −125.3 | −136.2 | −123.7 | −140.2 | −107.6 |
| | $NH_3$ | $Br^-$ | −131.6 | −114.8 | −126.7 | −114.3 | −132.3 | −99.6 |
| | | | (−126.7) | (−116.0) | | | | |
| | $NH_3$ | $I^-$ | −122.4 | −105.5 | −118.5 | −106.0 | −125.7 | −92.6 |
| | | | (−123.0) | (−106.7) | | | | |
| | $PH_3$ | $Cl^-$ | −153.8 | −142.2 | −142.0 | −131.2 | −145.2 | −122.3 |
| | | | (−154.0) | (−142.7) | | | | |
| | $PH_3$ | $Br^-$ | −142.2 | −130.7 | −131.9 | −121.1 | −136.0 | −113.0 |
| | | | (−142.4) | (−131.3) | | | | |
| | $PH_3$ | $I^-$ | −131.8 | −120.3 | −122.9 | −112.1 | −127.8 | −104.8 |
| | | | (−131.3) | (−120.3) | (−124.8) | (−112.7) | (−120.5) | (−105.9) |
| $[ML_2]^+ + L$ | $NH_3$ | | −32.3 | −16.0 | −26.1 | −14.6 | −27.8 | 2.4 |
| | $PH_3$ | | −31.7 | −19.4 | −24.2 | −12.7 | −31.9 | −7.9 |
| $[MXL] + L$ | $NH_3$ | $Cl^-$ | −18.5 | −3.1 | −13.8 | −2.4 | −12.1 | 13.8 |
| | $NH_3$ | $Br^-$ | −18.7 | −4.7 | −13.8 | −3.2 | −11.8 | 11.3 |
| | | | (−23.5) | (−5.9) | | | | |
| | $NH_3$ | $I^-$ | −18.8 | −6.2 | −13.7 | −3.8 | −11.6 | 9.2 |
| | | | (−20.5) | (−7.3) | | | | |
| | $PH_3$ | $Cl^-$ | −20.5 | −6.9 | −13.9 | −1.8 | −19.0 | 6.3 |
| | | | (−21.1) | (−7.4) | | | | |
| | $PH_3$ | $Br^-$ | −20.2 | −7.5 | −13.6 | −2.2 | −18.6 | 4.7 |
| | | | (−21.0) | (−8.2) | | | | |
| | $PH_3$ | $I^-$ | −19.9 | −8.3 | −13.2 | −2.6 | −18.1 | 3.3 |
| | | | (−20.1) | (−8.3) | (−13.5) | (−3.2) | (−23.0) | (2.3) |
| $[MX_2]^- + X^-$ | | $Cl^-$ | 33.2 | 57.4 | 21.8 | 41.1 | 33.8 | 56.1 |
| | | $Br^-$ | 33.3 | 53.0 | 25.5 | 43.1 | 31.7 | 57.1 |
| | | $I^-$ | 34.2 | 51.8 | 28.7 | 44.9 | 29.1 | 58.2 |
| $[MX_2]^- + L$ | $NH_3$ | $Cl^-$ | −8.3 | 14.3 | −5.2 | 11.1 | −0.7 | 24.3 |
| | $NH_3$ | $Br^-$ | −9.7 | 7.4 | −6.0 | 9.0 | −1.8 | 20.3 |
| | $NH_3$ | $I^-$ | −11.0 | 4.4 | −6.6 | 7.2 | −2.8 | 16.9 |
| | | | (−3.9) | (−0.1) | | | | |
| | $PH_3$ | $Cl^-$ | −15.0 | 7.3 | −7.5 | 8.2 | −13.5 | 12.1 |
| | $PH_3$ | $Br^-$ | −14.8 | 2.3 | −7.4 | 7.4 | −12.8 | 9.8 |
| | | | (−7.2) | (0.4) | | | | |
| | $PH_3$ | $I^-$ | −14.1 | 1.3 | −7.1 | 6.6 | −12.1 | 8.1 |
| | | | (−7.9) | (−0.6) | | | | |
| $[MXL] + X^-$ | $NH_3$ | $Cl^-$ | −50.9 | −34.0 | −52.7 | −39.6 | −51.2 | −21.9 |
| | $NH_3$ | $Br^-$ | −43.9 | −28.5 | −45.2 | −33.2 | −44.3 | −18.3 |
| | $NH_3$ | $I^-$ | −38.0 | −24.1 | −38.4 | −27.4 | −38.1 | −15.0 |
| | | | (−48.5) | (−28.6) | | | | |
| | $PH_3$ | $Cl^-$ | −58.9 | −44.4 | −56.9 | −43.8 | −54.7 | −29.0 |
| | $PH_3$ | $Br^-$ | −50.6 | −37.2 | −48.9 | −36.8 | −47.5 | −23.9 |
| | | | (−56.7) | (−39.1) | | | | |
| | $PH_3$ | $I^-$ | −43.4 | −31.2 | −41.7 | −30.4 | −41.0 | −19.4 |
| | | | (−48.7) | (−33.0) | | | | |

[a] The corresponding values for optimized structures are given in parentheses when possible.

geometries in which either the metal or the ligands are varied. Hence, we also carried out partial geometry optimization for all the explored complexes keeping the bond angles around the metal atom frozen (120° for tri-, 109.5° for tetracoordinate complexes). Even if calculations predict some charged complexes to be unstable in the gas phase, they may be stabilized by the dielectric environment. Besides, the structural and energetic results should be useful to describe trends and to understand the reasons for their instability.

**Interaction and Formation Energies.** The calculated interaction energy foran $ML_2$ fragment (bent to a bond angle of 120°) and an incoming ligand are summarized in Table 1, together with the formation energies corresponding to the optimized structure of the tricoordinate complexes (given in parentheses). We have also evaluated the effect that the presence of a dielectric environment has on the calculated interaction and formation energies of all tricoordinate Cu complexes studied (results provided as Supporting Information, Table S10), according to the CPCM approach (see the Methodology section). The interaction and formation energies for tetracoordinate complexes

are reported (Table 2) with fixed tetrahedral bond angles in all cases, as well as with optimized geometries (in parentheses) when possible. The energy contributions calculated for the frozen geometries are similar to those obtained for the optimized ones, except when the two structures are significantly different.

**Deformation Energies.** The energy of deformation of a linear [MAB] complex to the bent MAB fragment in a tricoordinate complex ($E_{def}$) can be decomposed as a sum of the *bending* and *stretching* energies ($E_{bend}$ and $E_{str}$ in Scheme 1, respectively). The bending energies for the complexes studied are given in Table 3. These values were obtained by bending the molecule to an A−M−B bond angle of 120° with fixed bond distances (as obtained in the optimization of the parent dicoordinate complex), whereas the stretching energies were calculated by allowing the bond lengths to relax after bending.[18] Given the

(18) If the order in which these two energy contributions are calculated is inverted, the resulting values are different, but the bending energy is always seen to be more important than the stretching one. Thus, in the rest of this paper, we adopt the convention of calculating always bending energies at the bond distances of the lower coordination number and the stretching energies at the bond angles of the higher coordination number.

**Table 2.** Calculated Interaction ($E_{int}$) and Formation ($E_f$) Energies between Tricoordinate Complexes and Neutral (L) or Anionic (X$^-$) Ligands (kcal/mol), with Bond Angles of 120° and 109.5°, Respectively[a]

| | L | X$^-$ | Cu | | Ag | | Au | |
|---|---|---|---|---|---|---|---|---|
| | | | $E_{int}$ | $E_f$ | $E_{int}$ | $E_f$ | $E_{int}$ | $E_f$ |
| **[ML$_3$]$^+$ + L** | NH$_3$ | | −21.4 | −12.5 | −18.1 | −12.3 | −16.7 | −4.9 |
| | PH$_3$ | | −24.1 | −14.6 | −17.3 | −9.7 | −22.4 | −7.1 |
| **[MXL$_2$] + X$^-$** | NH$_3$ | Cl$^-$ | −35.6 | −26.3 | −40.2 | −33.8 | −37.9 | −25.4 |
| | NH$_3$ | Br$^-$ | −30.0 | −21.5 | −33.5 | −27.3 | −31.6 | −20.1 |
| | NH$_3$ | I$^-$ | −25.2 | −17.0 | −27.6 | −21.5 | −26.3 | −15.9 |
| | | | (−35.0) | (−22.6) | | | | |
| | PH$_3$ | Cl$^-$ | −48.9 | −39.4 | −47.8 | −40.8 | −44.9 | −31.0 |
| | | | (−54.4) | (−42.0) | | | | |
| | PH$_3$ | Br$^-$ | −40.9 | −31.9 | −40.1 | −33.3 | −38.1 | −24.7 |
| | | | (−45.6) | (−34.4) | | | | |
| | PH$_3$ | I$^-$ | −34.2 | −25.6 | −33.4 | −26.8 | −32.1 | −19.2 |
| | | | (−37.9) | (−27.8) | | | | |
| **[MXL$_2$] + L** | NH$_3$ | Cl$^-$ | −11.1 | −3.3 | −8.9 | −4.2 | −5.6 | 3.3 |
| | | | (−17.8) | (−8.6) | | | | |
| | NH$_3$ | Br$^-$ | −11.5 | −3.9 | −9.1 | −4.4 | −5.7 | 3.0 |
| | | | (−16.5) | (−7.4) | | | | |
| | NH$_3$ | I$^-$ | −11.8 | −4.5 | −9.2 | −4.4 | −5.7 | 2.8 |
| | | | (−15.5) | (−7.2) | | | | |
| | PH$_3$ | Cl$^-$ | −15.3 | −7.0 | −9.7 | −3.6 | −12.6 | 0.5 |
| | | | (−17.0) | (−8.0) | (−11.5) | (−5.2) | (−17.6) | (−2.2) |
| | PH$_3$ | Br$^-$ | −15.3 | −7.2 | −9.6 | −3.7 | −12.4 | 0.3 |
| | | | (−16.4) | (−7.4) | (−11.0) | (−5.2) | (−18.1) | (−2.5) |
| | PH$_3$ | I$^-$ | −15.4 | −7.5 | −9.5 | −3.7 | −12.3 | 0.0 |
| | | | (−16.6) | (−7.7) | (−10.5) | (−4.5) | (−17.1) | (−1.1) |
| **[ML$_3$]$^+$ + X$^-$** | NH$_3$ | Cl$^-$ | −122.1 | −112.6 | −120.3 | −113.3 | −121.9 | −106.6 |
| | | | (−126.5) | (−117.9) | | | | |
| | NH$_3$ | Br$^-$ | −112.1 | −102.7 | −110.9 | −104.1 | −114.2 | −98.9 |
| | | | (−115.7) | (−107.4) | | | | |
| | NH$_3$ | I$^-$ | −103.4 | −94.0 | −102.6 | −95.8 | −107.6 | −92.2 |
| | | | (−106.9) | (−97.9) | | | | |
| | PH$_3$ | Cl$^-$ | −139.0 | −129.7 | −129.5 | −122.2 | −129.0 | −113.8 |
| | | | (−138.8) | (−131.3) | (−130.0) | (−123.7) | (−121.6) | (−116.5) |
| | PH$_3$ | Br$^-$ | −127.7 | −118.5 | −119.4 | −112.1 | −120.0 | −104.8 |
| | | | (−125.1) | (−118.7) | (−120.4) | (−113.6) | (−113.0) | (−107.6) |
| | PH$_3$ | I$^-$ | −117.6 | −108.4 | −110.4 | −103.1 | −112.0 | −96.9 |
| | | | (−114.8) | (−108.7) | (−112.3) | (−104.6) | (−105.4) | (−99.1) |
| **[MX$_2$L]$^-$ + X$^-$** | NH$_3$ | Cl$^-$ | 42.8 | 54.3 | 31.5 | 40.6 | 37.8 | 49.9 |
| | NH$_3$ | Br$^-$ | 43.7 | 54.8 | 34.5 | 43.4 | 40.1 | 51.7 |
| | NH$_3$ | I$^-$ | 43.6 | 54.2 | 36.9 | 45.5 | 41.6 | 52.8 |
| | PH$_3$ | Cl$^-$ | 35.3 | 47.7 | 27.6 | 37.1 | 31.8 | 46.2 |
| | PH$_3$ | Br$^-$ | 38.1 | 49.7 | 31.4 | 40.6 | 35.1 | 48.7 |
| | PH$_3$ | I$^-$ | 39.6 | 50.4 | 34.3 | 43.2 | 37.4 | 50.4 |
| | | | (36.0) | (49.2) | | | | |
| **[MX$_2$L]$^-$ + L** | NH$_3$ | Cl$^-$ | −4.6 | 4.5 | −3.0 | 3.4 | 1.6 | 10.3 |
| | NH$_3$ | Br$^-$ | −6.1 | 2.3 | −3.7 | 2.7 | 0.9 | 9.5 |
| | NH$_3$ | I$^-$ | −7.2 | 0.9 | −4.3 | 2.0 | −0.1 | 8.3 |
| | | | (−5.9) | (−1.3) | | | | |
| | PH$_3$ | Cl$^-$ | −11.6 | −1.8 | −5.7 | 1.3 | −7.8 | 4.3 |
| | | | (−9.3) | (−5.0) | | | | |
| | PH$_3$ | Br$^-$ | −11.5 | −2.2 | −5.6 | 1.2 | −7.6 | 3.9 |
| | | | (−9.6) | (−3.5) | | | | |
| | PH$_3$ | I$^-$ | −11.4 | −2.6 | −5.6 | 1.1 | −7.7 | 3.6 |
| | | | (−9.7) | (−3.3) | | | | |
| **[MX$_3$]$^{2-}$ + X$^-$** | | Cl$^-$ | 111.7 | 129.1 | 92.5 | 102.8 | 100.3 | 116.6 |
| | | | (111.7) | (129.1) | | | | |
| | | Br$^-$ | 107.8 | 125.1 | 94.0 | 104.9 | 97.2 | 108.0 |
| | | | (107.8) | (125.1) | (94.0) | (104.9) | | |
| | | I$^-$ | 103.0 | 119.5 | 92.4 | 105.1 | 98.1 | 109.9 |
| | | | | | (92.4) | (105.1) | (95.6) | (108.3) |
| **[MX$_3$]$^{2-}$ + L** | NH$_3$ | Cl$^-$ | −2.0 | 11.2 | −0.4 | 10.6 | 4.6 | 16.1 |
| | NH$_3$ | Br$^-$ | −3.9 | 9.2 | −1.6 | 9.2 | 3.4 | 14.9 |
| | NH$_3$ | I$^-$ | −5.8 | 6.9 | −2.7 | 7.8 | 2.0 | 13.6 |
| | PH$_3$ | Cl$^-$ | −14.9 | −2.4 | −5.6 | 4.6 | −11.5 | 0.1 |
| | PH$_3$ | Br$^-$ | −13.4 | −1.1 | −5.2 | 4.9 | −10.3 | 1.3 |
| | PH$_3$ | I$^-$ | −12.0 | −0.1 | −4.8 | 5.0 | −9.3 | 2.5 |
| | | | (−6.8) | (−2.9) | | | | |

[a] The values for optimized structures are given in parentheses.

small values of the stretching energies and the relationship between bending and deformation energies, we show in Table 3 only $E_{bend}$, while the deformation and stretching energies are provided as Supporting Information (Table S11). The pyrami-

dalization energies calculated for tricoordinate ML$_3$ and MXL$_2$ fragments (L = NH$_3$ or PH$_3$, X = Cl, Br, or I) in the optimized tetracoordinate complexes are collected in Table 4 (stretching energies provided as Supporting Information, Table S12).

**Table 3.** Calculated Energies Required for Bending (kcal/mol) Linear [MAB] Complexes to a Bond Angle of 120°

| A | B | Cu | Ag | Au |
|---|---|---|---|---|
| $NH_3$ | $NH_3$ | 17.5 | 13.2 | 34.1 |
| $PH_3$ | $PH_3$ | 11.0 | 10.7 | 22.3 |
| Cl | $NH_3$ | 15.7 | 12.5 | 28.0 |
| Br | $NH_3$ | 14.3 | 11.5 | 25.0 |
| I | $NH_3$ | 12.8 | 10.5 | 22.8 |
| Cl | $PH_3$ | 12.9 | 12.4 | 24.9 |
| Br | $PH_3$ | 12.0 | 11.5 | 22.7 |
| I | $PH_3$ | 10.8 | 10.6 | 20.8 |
| Cl | Cl | 22.3 | 16.5 | 25.6 |
| Br | Br | 16.8 | 15.0 | 22.4 |
| I | I | 15.0 | 13.8 | 19.9 |

**Table 4.** Calculated Pyramidalization Energy (kcal/mol) for [MABC] Trigonal Complexes to Tetrahedral Angles

| A | B | C | Cu | Ag | Au |
|---|---|---|---|---|---|
| $NH_3$ | $NH_3$ | $NH_3$ | 8.7 | 5.6 | 11.7 |
| $PH_3$ | $PH_3$ | $PH_3$ | 8.7 | 6.9 | 14.8 |
| Cl | $NH_3$ | $NH_3$ | 7.5 | 4.4 | 8.7 |
| Br | $NH_3$ | $NH_3$ | 7.2 | 4.4 | 8.5 |
| I | $NH_3$ | $NH_3$ | 7.0 | 4.5 | 8.3 |
| Cl | $PH_3$ | $PH_3$ | 7.9 | 5.8 | 12.7 |
| Br | $PH_3$ | $PH_3$ | 7.5 | 5.6 | 12.3 |
| I | $PH_3$ | $PH_3$ | 7.3 | 5.5 | 11.9 |
| Cl | Cl | $NH_3$ | 8.5 | 5.8 | 8.2 |
| Br | Br | $NH_3$ | 8.2 | 5.9 | 8.3 |
| I | I | $NH_3$ | 7.9 | 6.0 | 8.4 |
| Cl | Cl | $PH_3$ | 9.5 | 6.8 | 11.6 |
| Br | Br | $PH_3$ | 9.0 | 6.7 | 11.1 |
| I | I | $PH_3$ | 8.5 | 6.5 | 10.9 |
| Cl | Cl | Cl | 12.2 | 10.0 | 10.7 |
| Br | Br | Br | 12.0 | 9.8 | 10.7 |
| I | I | I | 11.5 | 9.6 | 10.9 |

**Ligand Preorganization Energies.** In all the cases studied here, the ligand preorganization does not significantly contribute to the formation energy. Ligand preorganization applies only to polyatomic ligands (here $PH_3$ and $NH_3$), and for these, it is found that the changes required in bond angles and distances upon coordination are minimal, resulting in preorganization energies of at most 2.0 kcal/mol.

## Discussion

**Structural Aspects.** The calculated bond distances are in good agreement with the experimental data (Figure 2; data provided as Supporting Information, Tables S4–S8 and S14). To avoid tedious comparisons of the large number of bond distances considered, we focus only on the ranges of calculated and experimental M−Z distances in [$ML_{n−1}Z$] complexes for each choice of metal ion, coordination number ($n = 2$−4), and donor atom (Z = N, P, Cl, Br, I). For a given M−Z distance and coordination number $n$, the ranges shown comprise calculated and experimental values for all [$ML_{n−1}Z$] compounds. The main source of variability of the calculated M−Z distances (horizontal error bars) comes from differences found in [$MX_n$] (X = halide) compared to [$MXL_{n−1}$] (L = $NH_3$, $PH_3$; $n = 3, 4$) complexes, whereas M−L distances in [$MXL_{n−1}$] vary very little with the halide. On the other hand, the major source of variance in the experimental data comes from the different degrees of bending (in tricoordinate complexes) or pyramidality (in tetra-coordinate complexes), since bond distances are highly sensitive to those angles.[19] It must be noted that the M−N and M−P

bond distances within a family of [$MX_mL_n$] compounds (L = $NH_3$, $PH_3$) are practically insensitive to the nature of X for a given coordination number. Variations of bond distances with the coordination number will be discussed below.

The calculated bond distances follow these general trends: (1) For the same set of ligands, the metal−ligand distances increase in the order Cu < Au < Ag. (2) For the same metal and similar set of ligands, a given metal−ligand distance increases with coordination number, roughly 0.1 Å per each additional ligand present. (3) The M−X distances increase in the order Cl < Br < I for the same metal and analogous accompanying ligands.

Whenever the optimized structure of a complex of type [$MA_2B$] gives A−M−B bond angles significantly smaller than 120°, the M−B bond distance is larger than that in the frozen geometry with bond angles of 120°. To give just one example, we focus on [$CuI_2(NH_3)$]⁻, for which the optimized I−Cu−N bond angle is 103° and the Cu−N distance 2.251 Å to be compared with 2.119 Å at 120°. Such a structural result is a consequence of the softness of the potential energy surface for the association reaction and of the correlation between bond angle and bond distance along that path, illustrated by the small variation of the interaction energy between [$Cu(PH_3)_2$]⁺ and I⁻ with the P−Cu−P angle (Figure 3a). We can also see (Figure 3b) that the optimized Cu−I distance is correlated with the P−Cu−P bond angle in a nearly linear way between 120° and 180°, decreasing by nearly 0.1 Å when P−Cu−P = 120°. A similar correlation is found between experimental bond angles and distances in the analogous compounds [$MX(PR_3)_2$] (M = Cu, Au; X = Cl, Br, I), as well as for other families (plots provided as Supporting Information, Figure S2).

From the results of geometry optimization on complexes of general formula [$MCl(EMe_3)_2$] with more realistic amine and phosphine ligands (M = Cu, Ag, or Au and E = N or P; data provided as Supporting Information, Table S9), several observations can be made: (i) substitution of the hydrogen-donor ligands $EH_3$ by the methylated analogues $EMe_3$ converts computationally unstable complexes into stable ones in the gas phase (M = Cu, E = N and M = Ag or Au, E = P); (ii) the calculated geometry for [$CuCl(NH_3)_2$] with frozen bond angles and the optimized geometry for [$CuCl(NMe_3)_2$] are reasonably similar; (iii) the optimized geometries for [$AgCl(PMe_3)_2$] and [$AuCl(PMe_3)_2$] present nearly linear M($PMe_3$)$_2$ skeletons with the chloro ligand at a relatively long distance, in good agreement with the large variability found in experimental bond distances and angles as well as with the soft potential well that results from the angle dependence of the bending and interaction energies.

If we turn now to tetracoordinate [$MZL_3$] complexes, we can also see in their optimized structures that the large variability of experimental distances and angles with the ligands is due in part to the varying degree of pyramidalization of the $ML_3$ fragments, since there is a correlation between bond distance and pyramidality angle. This can be illustrated for the large family of [$CuXL_3$] complexes (where X is Cl or I, and L is any ligand with a donor atom belonging to groups 14−16), for which the Cu−X bond distance decreases as the pyramidality (indicated

(19) Liu, X.-Y.; Mota, F.; Alemany, P.; Novoa, J. J.; Alvarez, S. *Chem. Commun.* **1998**, 1149.
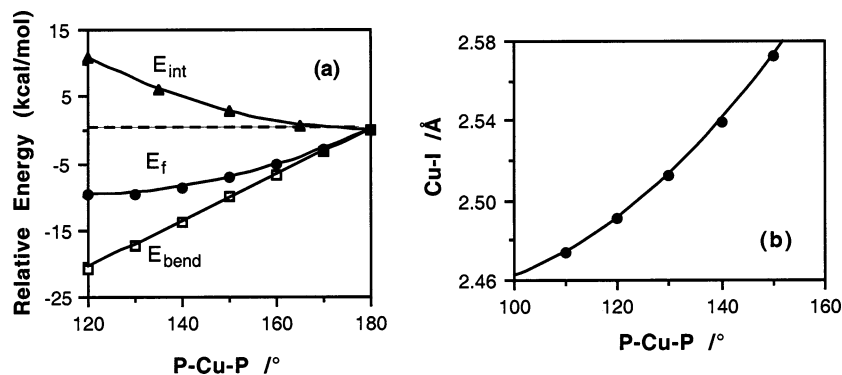
**Figure 3.** Variation with the P−Cu−P bond angle of (a) the energy contributions and (b) the Cu−I bond distance in [CuI(PH$_3$)$_2$].
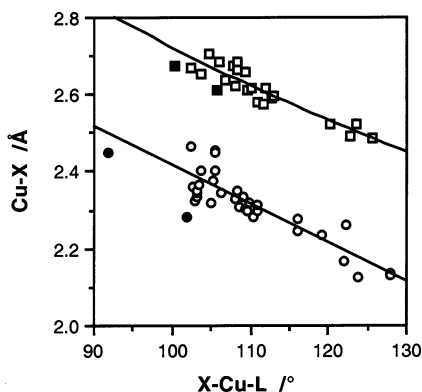


**Figure 4.** Experimental Cu−X bond distances (X = Cl, open circles; X = I, open squares) in tetracoordinate [CuXL$_3$] complexes as a function of the pyramidality (L is any ligand with a donor atom belonging to groups 14−16). The calculated values for L = NH$_3$ and PH$_3$ are also shown (closed symbols).

by the average X−Cu−L bond angle, α) increases, both for the experimental and the theoretically optimized structures (Figure 4). The same qualitative behavior is found for Ag and Au complexes, although with poorer correlations. In particular, it can be seen that the longest M−X distances are associated with pyramidality angles α of around 80° (found in cubane clusters in which the metal and halide are occupying neighboring vertexes), intermediate distances are found for mononuclear complexes with monodentate ligands (α values of around 90°−112°), and the shortest distances are found with tridentate ligands that have α values larger than 115°. Interestingly, this behavior is revealed by comparing the optimized and frozen structures of [AgCl(NH$_3$)$_3$]: the former presents N−Ag−Cl angles of 83° at a quite long Ag−Cl distance (2.706 Å), in contrast with the frozen structure with tetrahedral angles that presents a much shorter distance (2.499 Å).

As examples of how such a large variability in the pyramidality angle and in M−X distances is also found experimentally, let us just give a couple of examples of gold complexes. Thus, a compound with a trisphosphine[20] ligand is the only one that has a pyramidality angle larger than 105° (α = 118°) due to the tridentate nature of the phosphine ligand. Such a large degree of pyramidalization is associated to a remarkably short Au−Cl distance of 2.512 Å, whereas all other compounds in the same family have distances in excess of 2.71 Å, the extreme case being that of a calixarene phosphine complex[21] with α = 91°

and a long Au−Cl bond distance (3.01 Å). Similarly, a silver complex with a tridentate phosphine[22] has a quite short Ag−I distance (2.69 Å) at α = 126°, whereas all other Ag−I distances in [AgI(PR$_3$)$_3$] complexes are longer than 2.85 Å, consistent with much less pyramidalized AgP$_3$ fragments (α < 123°).

We can analyze now how the metal−ligand bond distances change with the metal atom, the ligand, or the coordination number. To that end, we compare bond distances within a series of homoleptic complexes (data provided as Supporting Information, Table S13). In general, for the same ligand, the bond distances increase in the same order found above for tricoordinate complexes: Cu−L < Au−L < Ag−L, in agreement with crystallographic studies that showed the atomic radius of Au to be smaller than that of Ag,[23,24] a fact that is reflected also in the atomic radii determined from a structural database analysis.[25] For the same metal atom, on the other hand, the metal−ligand bond distances follow the order I > Br > Cl > P > N. Finally, a clear dependence of a given metal−ligand bond distance on the coordination number appears, with an increase of roughly 0.1−0.2 Å per each ligand added.

**Interaction Energies.** According to the results for tricoordinate complexes (Table 1), the order of magnitude of the interaction energy in the gas phase is mostly determined by the net charges of the two interacting fragments (Figure 5a), as could be expected from simple electrostatic considerations. Thus, the largest attractive (negative) interaction energies are those of [ML$_2$]$^+$ + X$^-$ ionic pairs. Also the attractive ion−dipole interactions of type [ML$_2$]$^+$ + L and [MXL] + X$^-$ are more stabilizing than those between two neutral fragments [MXL] and L, while the anion−dipole interactions of type [MX$_2$]$^-$ + L are clearly destabilizing. Finally, the anion−anion interactions are seen to be strongly destabilizing, as expected from purely electrostatic arguments. In summary, the interaction energies between neutral species can in principle be taken as an indication of a purely electronic interaction devoid of ionic components. A word of caution must be said, though, because the presence of solvent molecules in solution, or of counterions in the crystal, may significantly affect the relative energies of reactants and products, an issue that will be analyzed below.

(20) Zank, J.; Schier, A.; Schmidbaur, H. *J. Chem. Soc., Dalton Trans.* **1999**, 415.

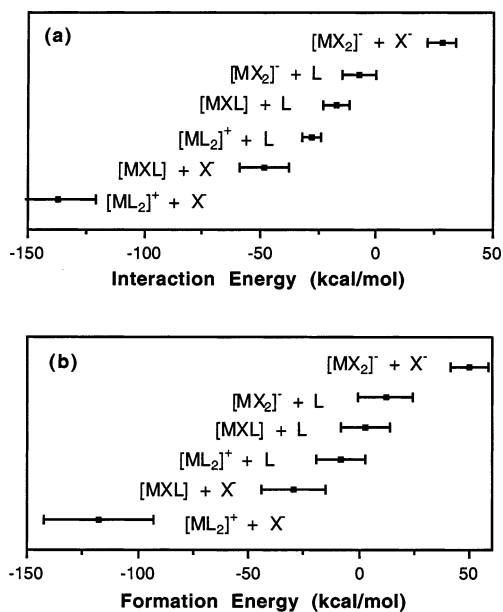(21) Dieleman, C. B.; Matt, D.; Harriman, A. *Eur. J. Inorg. Chem.* **2000**, 831.
(22) Camalli, M.; Caruso, F. *Inorg. Chim. Acta* **1990**, *169*, 189.
(23) Bayler, A.; Schier, A.; Bowmaker, G. A.; Schmidbaur, H. *J. Am. Chem. Soc.* **1996**, *118*, 7006.
(24) Tripathi, U. M.; Bauer, A.; Schmidbaur, H. *J. Chem. Soc., Dalton Trans.* **1997**, 2865.
(25) Palacios, A. A.; Aullón, G.; Alemany, P.; Alvarez, S. *Inorg. Chem.* **2000**, *39*, 3166.

**Figure 5.** Scatterplot of the ranges of calculated (a) interaction energies and (b) formation energies for families of ligand association reactions to dicoordinate complexes (Table 1). The error bars indicate the ranges of values found within each family.

Let us now analyze the trends in interaction energies within a family of tricoordinate compounds by looking at the gas-phase results (Table 1). Some general results can be outlined: (i) Interaction with phosphines (eqs 5.2, 5.4, and 5.6) is more favored than with ammonia in most cases, the exceptions corresponding to the association of one of these two ligands with a dicoordinate Ag complex. (ii) For similar reactions of association of a halide (eqs 5.1 and 5.3), the strength of interaction follows the sequence Cl > Br > I. (iii) Interaction with a phosphine ligand is in general more stabilizing with Cu than with Ag or Au. (iv) The only interactions that appear to be destabilizing in the gas phase are those between an anionic complex and an anionic ligand (eq 5.5).

Our results for tetracoordination (Table 2) also show that the largest part of the calculated interaction energy is dominated by the net charges of the interacting fragments. If we analyze the trends in interaction energies within one family of tetracoordinate compounds, the following general observations can be made: (i) Interaction of halide-containing complexes with phosphine (eqs 6.4, 6.6, and 6.8) is more favorable than with ammonia, while the formation of homoleptic tetracoordinate complexes (eq 6.2) is more favorable for phosphine when the metal is Au and for ammonia when the metal is Cu, whereas the two neutral ligands interact similarly with Ag. (ii) For similar reactions of association of a halide (eqs 6.1, 6.3, and 6.5), the stabilizing character of the interaction energy decreases according to the sequence Cl > Br > I, as found above for tricoordinate complexes. (iii) No clear trend is found for the dependence of the interaction energy on the nature of the metal, although it must be stressed for the subsequent discussion that the interaction energies for Au are in general comparable to those for Cu and Ag. (iv) The interactions between anionic complexes and anionic ligands (eq 6.5 and 6.7) appear to be destabilizing in the gas phase, while interactions between $[AuX_2(NH_3)]^-$ complexes and ammonia are very weak.

**Deformation Energies.** The reorganization of the metal coordination sphere on going from a linear (A−M−B bond angle of 180°) to a trigonal planar (A−M−B = 120°) $d^{10}$ complex ($E_{def}$ step in Scheme 1) is seen to be destabilizing (Table 3) and should be expected to be an important factor in determining the overall formation energy and therefore the equilibrium constant of the ligand association reaction (eq 1). The stretching energies (Supporting Information, Table S11) are relatively small in all cases compared to the bending energies. Consequently, the deformation energy ($E_{def}$ in Scheme 1) is essentially determined by the bending component, which accounts for at least an 85% of the deformation energy. Therefore, we will not consider the stretching energy in subsequent discussions. Even if one would expect a bond angle distortion to require less energy than stretching a bond (think on the bending and stretching force constants and vibrational frequencies, for instance), it must be stressed that the changes in bond angles (ca. 60°) are much larger than those in bond distances (ca. 0.1 Å) when going from a linear dicoordinate to a trigonal tricoordinate complex.

To see how the bending energies (Table 3) are affected by the choice of metal and ligands, we show for several complexes the variation of that energy contribution as a function of the bond angle around the metal while the rest of the molecule is kept rigid (Figures 6 and 7). In Figure 6, it can be seen that the bending energy for a given set of ligands is practically identical for Cu and Ag but significantly larger for Au (by nearly a factor of 2). Concerning the effect of the ligand, we observe (Figure 7) that phosphine complexes are more easily bent than amine derivatives, and softer halides offer less resistance to bending than harder ones (bending energies decrease in the order Cl > Br > I).

Concerning the deformation energy of a tricoordinate complex required to associate a fourth ligand, the changes in bond length represent a minor energy contribution (stretching energies provided as Supporting Information, Table S12) and the reorganization energy of the coordination sphere is mostly associated to changes in bond angles, the pyramidalization component accounting for at least a 64% of the energy of deformation. We note also that the stretching component is significative only when the entering ligand is a halide (up to 6 kcal/mol) and much smaller (0.8 kcal/mol) when the entering ligand is ammonia or phosphine. In Table 4, we can see that, for a given set of ligands, the pyramidalization energy increases in the following order: Ag < Cu < Au. Also some dependence on the nature of L is observed, the pyramidalization energies being smaller for amino than for phosphino complexes, although the effect of the metal is seen to be more important. It is also interesting to note that the energy required for the pyramidalization of a given tricoordinate complex is always smaller than that required to bend the dicoordinate parents (about one-half in average).

Let us now discuss the deformation energies of tricoordinate complexes. For the six homoleptic $[ML_3]^+$ complexes (L = $NH_3$ and $PH_3$), we have calculated the pyramidalization energy as a function of the degree of pyramidalization, measured by the angle between the M−L bonds and the principal axis of the molecule (Figure 8). We can see that for significant deviations from planarity the distortion requires always more energy for Au than for Ag and Cu, the diference being larger for $PH_3$ than for $NH_3$. A relatively surprising result is that also for Cu the pyramidalization energies are larger than for Ag. This is most
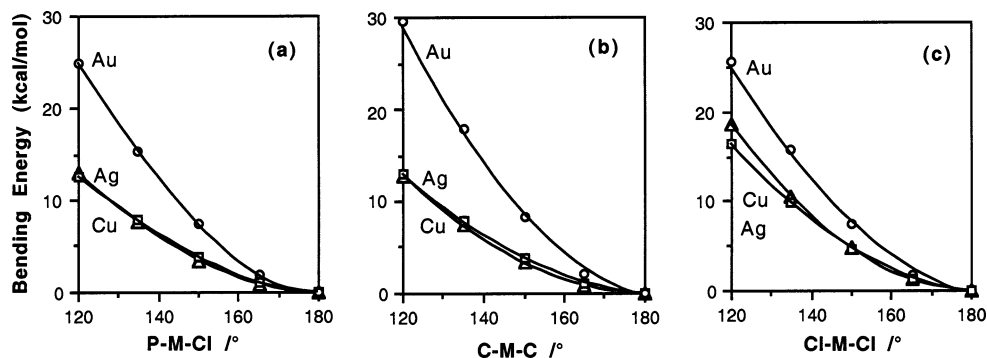
**Figure 6.** Calculated bending energies as a function of the bond angles in dicoordinate d[10] complexes: (a) [MCl(PH₃)], (b) [M(CNH)₂]⁺, and (c) [MCl₂]⁻, where M = Cu (△), Ag (□), and Au (○).
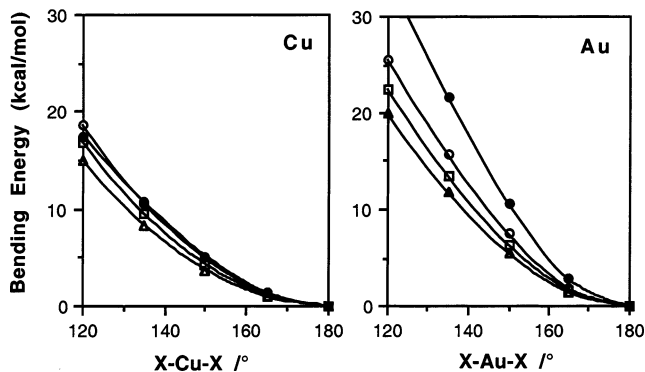


**Figure 7.** Bending energies as a function of the bond angle with different ligand sets for Cu[I] and Au[I] complexes: [M(NH₃)₂]⁺ (●); [MCl₂]⁻ (○); [MBr₂]⁻ (□); [MI₂]⁻ (△).

likely due to steric repulsions between ligands, since the shorter Cu—L bond distances result in shorter ligand···ligand contacts.

**Formation Energies of Tricoordinate Complexes.** The analysis of the calculated formation energies of tricoordinate complexes (Table 1) reveals interesting trends:

(1) The fact that the range of formation energies for each family of tricoordinate complexes resembles that of the corresponding interaction energies (Figure 5b and 5a, respectively) indicates that also the calculated gas phase formation energies are mostly controlled by the net charges. Nevertheless, there is a significant variation in the interaction and formation energies within a given family (error bars in Figure 5) that must be associated with the nature of the metal and ligands involved.

(2) The formation energies are shifted to more positive values relative to the corresponding interaction energies, consistent with the importance of the destabilizing bending contribution.

(3) The trends found for the interaction energies are reproduced by the formation energies only for reactions 5.1, 5.5, and 5.6 but not for reactions 5.2, 5.3, and 5.4.

(4) There is an excellent correlation between formation energies and the sum of the corresponding interaction and bending energies,[26] the only reactions that deviate from the general trend being [AuX₂]⁻ + X⁻.

(5) The less stable tricoordinate complexes among the group 11 metals correspond to Au; in particular, [Au(NH₃)₃]⁺ and all complexes of the [AuXL₂] family are predicted to be unstable toward dissociation in the gas phase with the loss of one phosphine or amine ligand. Such a result seems to be in

contradiction with the existence of crystallographically characterized halobisphosphine Au[I] compounds, as reflected in the structural data (deposited as Supporting Information, Table S5). A closer look at those experimental structures, though, reveals that they are far from the trigonal planar geometry assumed in our frozen geometry calculations, the P—Au—P bond angles appearing in the range 130°–173°. It is thus clear that the experimental bond angles represent a compromise between the small values required for a strong interaction with the incoming ligand and the large values compatible with a small bending energy. A different case is that of a complex with a bidentate diphosphine,[27] which should present an extra stability toward dissociation due to the chelate effect.

(6) The only other family of tricoordinate complexes that is predicted by calculations to be unstable in the gas phase is that of the [MX₃]²⁻ anions, an intriguing result if we consider the existence of many salts of the copper and silver anions whose crystal structures have been solved. This apparent disagreement between calculations and experiment is most likely due to the neglect of the Madelung potential that results in an overestimation of the net electrostatic interaction between two interacting anions, as pointed out by Boldyrev et al.[28]

All the above results are for the gas phase, and caution must be taken when comparisons are done with experimental results obtained in solution because of the influence that the solvent may have on the formation energies involving charged species. It is thus appropriate to discuss here our results for tricoordinate Cu complexes including a dielectric environment (data in Table S10, Supporting Information). To illustrate such a discussion, we show in Figure 9 the ranges of formation energies calculated in the gas phase and in the most stabilizing solvent for each family of ligand association reactions to Cu dicoordinate complexes (water in all cases except for the bottom two reactions). The analysis of our results can be summarized as follows:

(1) Unsurprisingly, the dielectric environment affects in a different way the formation energies of the studied complexes depending on the net charges of the interacting and the resulting species: (a) interactions between a neutral complex and an incoming neutral ligand are practically unaffected; (b) interactions between an anionic ligand and a neutral or cationic complex are less stabilizing in the presence of a dielectric than in the gas phase, with a less polar solvent such as dichlo-

---

(26) Least-squares fitting of all values in Tables 1 and 3 gives $E_f = -0.164 + 1.006 (E_{int} + E_{bend})$, regression coefficient $r^2 = 0.999$ for 66 data sets.

(27) Viotte, M.; Gautheron, B.; Kubicki, M. M.; Mugnier, Y.; Parish, R. V. *Inorg. Chem.* **1995**, *34*, 3465.

(28) Boldyrev, A. I.; Gutowski, M.; Simons, J. *Acc. Chem. Res.* **1996**, *29*, 497.
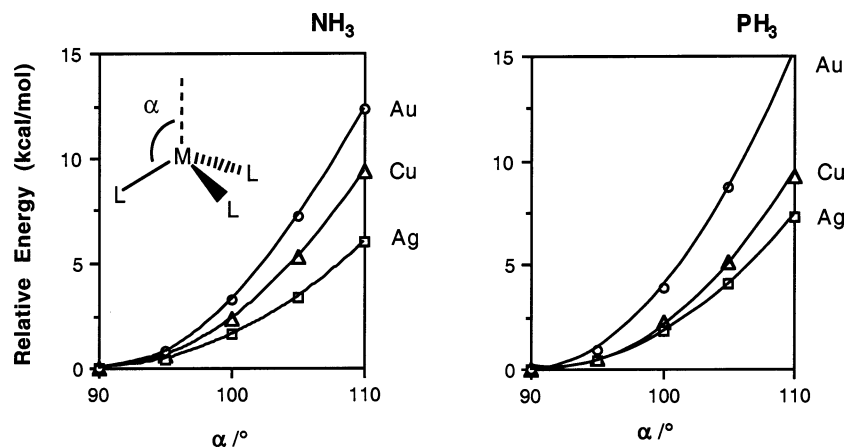
**Figure 8.** Energy of pyramidalization of tricoordinate [ML$_3$]$^+$ complexes as a function of the degree of pyramidalization $\alpha$ for L = NH$_3$ (left) and PH$_3$ (right).
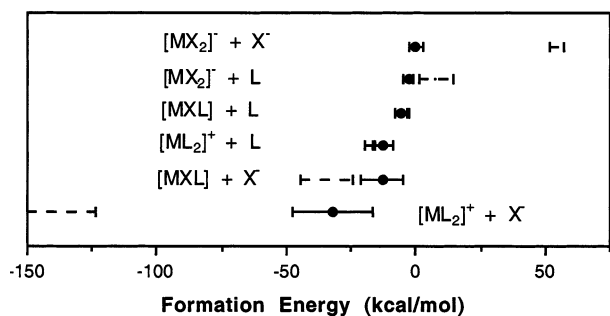


**Figure 9.** Scatterplot of the ranges of calculated formation energies for ligand association to a dicoordinated Cu complex in the most stabilizing solvent (water or dichloromethane, solid bars) and in the gas phase (black dashed bars) classified by the net charge of the interacting species.

romethane being more favorable for the formation of the tricoordinate complex than water; (c) interactions between an anionic complex and neutral or anionic ligands, which are disfavored in the gas phase, can become slightly favorable in an aqueous environment; and (d) interactions between a cationic complex and a neutral ligand are more favorable in the gas phase than in the presence of a solvent.

(2) Highly interesting for the qualitative approach of the present work, which focuses more on trends than on numeric values, consideration of the dielectric environment does not affect the trends of the gas-phase formation energies (i.e., their dependence on the nature of X, L, and M) for a given type of reaction (eqs 5.1−5.6), except for the dependence of reactions 5.5 on the nature of X and of reactions 5.6 on the nature of L, for which the stability order is inverted from gas phase to water solution.

(3) Good qualitative information on relative stabilities in solution can be extracted from the formation energies in the gas phase, except for ligand association reactions involving an anionic [MX$_2$]$^-$ complex.

**Ligand Substitution and Dimerization Reactions of Tricoordinate Complexes.** Some ideas about reactivity can also be deduced from the calculated formation energies. Given the small energies of formation of [AgXL$_2$] complexes through ligand association to [AgXL], the corresponding di- and tricoordinate complexes should be expected to be in equilibrium. On the other hand, the interaction and formation energies calculated for the reaction between a neutral complex and an anionic ligand (eq 5.3) suggest that the resulting tricoordinate

complexes should be stable. However, since the formation of the same complexes from [MX$_2$]$^-$ and L (eq 5.6) are thermo-dynamically unfavorable (positive values of $E_f$ in Table 1), one should expect the former reaction to ultimately give place to ligand substitution, as indicated in eq 7.

$$[MXL] + X^- \rightarrow [MX_2L]^- \rightarrow [MX_2]^- + L \qquad (7)$$
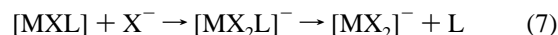
However, we could expect that ligand association reactions 5.6 which are slightly unfavorable in the gas phase might lead to the isolation of the tricoordinate [MX$_2$L]$^-$ complexes in aqueous solution (data in Table S10, Supporting Information). As a consequence, we can expect to find Cu or Ag complexes of this family but not Au analogues; phosphine complexes are more likely than amine ones, and iodo and bromo complexes are more likely than chloro ones. In agreement with such predictions, a database search tells us that structurally charac-terized Cu compounds of the [MX$_2$L]$^-$ stoichiometry are rather common (67 structures found, 46 with phosphines and 21 with amines), whereas Ag complexes are scarcer (eight with phos-phine and two with amine ligands) and no Au complexes of that stoichiometry were found. Most of the tricoordinate CuX$_2$L and AgX$_2$L units are actually found in dinuclear complexes with two halo bridges, some exceptions corresponding to the mono-nuclear copper dihalophosphine complexes.[29,30] A few other mononuclear complexes are found, but these have relatively large bond angles, as in an AgBr$_2^-$ moiety[31] with a Br−Ag−Br bond angle of 154° and a weakly coordinated pyridyl ring or in dichloro- and dibromothiamine Cu$^I$ complexes with N−Cu−X bond angles of around 135° and one long Cu−X distance.[32,33] The present results suggest that these dimers are probably formed by a dimerization reaction of two dicoordinate molecules (reaction **1**, formally analogous to the association of a neutral ligand to a neutral complex), rather than through reaction between a tricoordinate complex and a monocoordinate one (reaction **2**). However, we cannot rule out a more elaborate

(29) Bowmaker, G. A.; Skelton, B. W.; White, A. H.; Healy, P. C. *J. Chem. Soc., Dalton Trans.* **1988**, 2825.
(30) Bowmaker, G. A.; Wang, J.; Hart, R. D.; White, A. H.; Healy, P. C. *J. Chem. Soc., Dalton Trans.* **1992**, 787.
(31) Tulloch, A. A. D.; Danopoulos, A. A.; Winston, S.; Kleinhenz, S.; Eastham, G. *J. Chem. Soc., Dalton Trans.* **2000**, 4499.
(32) Cramer, R. E.; Maynard, R. B.; Evangelista, R. S. *J. Am. Chem. Soc.* **1984**, *106*, 111.
(33) Archibong, E.; Adeyemo, A.; Aoki, K.; Yamazaki, H. *Inorg. Chim. Acta* **1989**, *156*, 77.
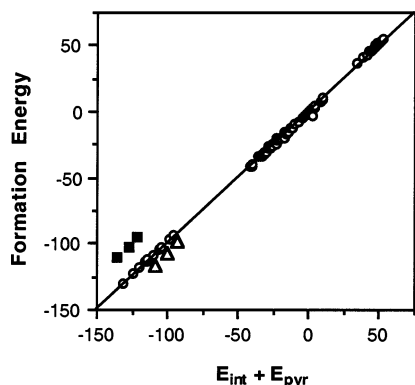
**Figure 10.** Calculated formation energies of tetracoordinate complexes by ligand association as a function of the sum of the interaction and pyramidalization components (kcal/mol). Reactions that deviate from the general trend are [AuX(NH$_3$)$_2$] + X$^-$ (■) and [AuX(NH$_3$)$_2$] + X$^-$ (△), with X = Cl, Br, or I.

mechanism (e.g., reaction **3**) involving a dinuclear species with one tricoordinate and one tetracoordinate intermediate, since structurally characterized examples of this type of compounds are well-known.
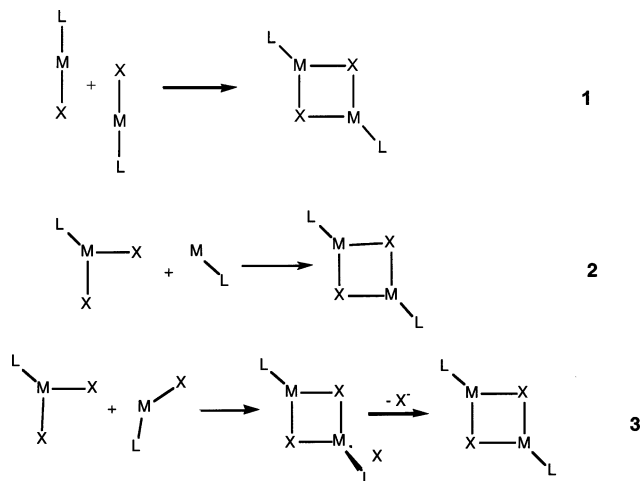


**Formation and Interaction Energies of Tetracoordinate Complexes.** Focusing now on the calculated formation energies of tetracoordinate compounds in the gas phase (Table 2), we find again that the net charges of the interacting species are very important in determining the interaction energy. In addition, the following observations can be made:

(1) For the reactions 6.1, 6.3, and 6.5 the formation energies decrease in the order Cl > Br > I for all three metals, and the same trend is found for the interaction energies.

(2) The formation energies are determined mostly by the interaction and pyramidalization components as seen in Figure 10, where the linear least-squares fitting[34] represents quite accurately the general behavior. Only the reactions [AuL$_3$] + X$^-$ deviate from the general behavior, although still an excellent correlation between $E_f$ and the sum of interaction and pyramidalization energy is found within each family.

(3) Several groups of tetracoordinate compounds are predicted to be unstable toward dissociation. Even if tetracoordinate metals with those stoichiometries have been structurally characterized,

a closer look will show that the prediction of instability of several complexes is consistent with the available structural data:

(a) The [MX$_2$L$_2$]$^-$ complexes are predicted to dissociate one neutral ligand L, except for M = Cu and L = PH$_3$. Although many structures of complexes with two halides and two amines or phosphines have been determined experimentally (as reflected in the structural data provided as Supporting Information, Table S8), practically all have two bridging halo ligands. One exception corresponds precisely to the mononuclear [CuI$_2$(PPh$_3$)$_2$]$^-$ complex,[35] the only member of this family predicted to be stable. The other exceptions are two Au compounds which have a nearly linear P−Au−P group (bond angles of ∼160°).[36] From the discussion above, it is clear that the unfavorable formation energy calculated for complexes with tetrahedral angles can be made favorable by restraining the deformation of the precursor complex, thus lowering this destabilizing energy contribution. As an example, the formation energy of [CuI$_2$(NH$_3$)$_2$]$^-$ is positive when the frozen geometry is considered, whereas in its optimized geometry it presents a negative formation energy. A closer inspection of the optimized structure shows that it is strongly distorted from the tetrahedral geometry. The fact that [MX$_2$L$_2$]$^-$ complexes are unstable toward dissociation of L seems to be in contradiction with the presence of MX$_2$L$_2$ groups in dinuclear complexes, but test calculations for [AgCl$_2$(PH$_3$)$_2$]$^-$ show that ligand dissociation is unfavorable (**5**, $E_f = -4.5$ kcal/ mol), in contrast with the corresponding reaction for the mononuclear complex (**4**, $E_f = 4.6$ kcal/mol, Table 2). Energy
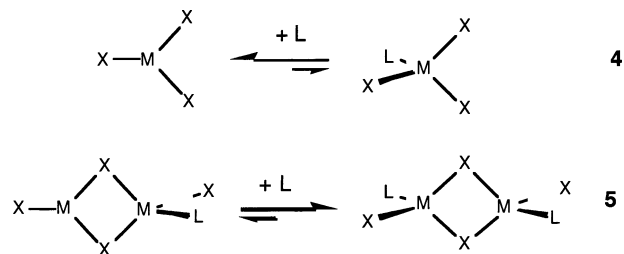


decomposition indicates that the interaction of PH$_3$ with the dinuclear complex is significantly more stabilizing than with the mononuclear one ($E_{int} = -12.2$ and $-5.7$ kcal/mol, respectively), in agreement with the existence of dinuclear but no mononuclear complexes of this stoichiometry, although further theoretical work is required to find an explanation for such results.

(b) Compounds of the type [MX$_3$L]$^{2-}$ are expected to dissociate one neutral ligand L, except for [AgCl$_3$(PH$_3$)]$^{2-}$. Again, all Cu and Ag compounds of this family that have been structurally characterized present at least two halide bridges, among which cubane tetramers with triple bridges are quite common. No Au compounds of this family seem to have been structurally characterized.

(c) The [AuX(NH$_3$)$_3$] complexes, at difference with the Cu and Ag analogues, are predicted to dissociate one NH$_3$. Consistently, no structures have been found with one halo and three amine ligands.

(d) The [AuX(PH$_3$)$_3$] and [AgI(PH$_3$)$_3$] complexes are predicted to dissociate two phosphines. Some of the structurally

(34) Least-squares fitting: $E_f = 0.927 + 1.001$ ($E_{int} + E_{pyr}$); regression coefficient $r^2 = 0.999$ for 126 ligand association reactions.

(35) Bowmaker, G. A.; Camus, A.; Healy, P. C.; Skelton, B. W.; White, A. H. *Inorg. Chem.* **1989**, *28*, 3883.
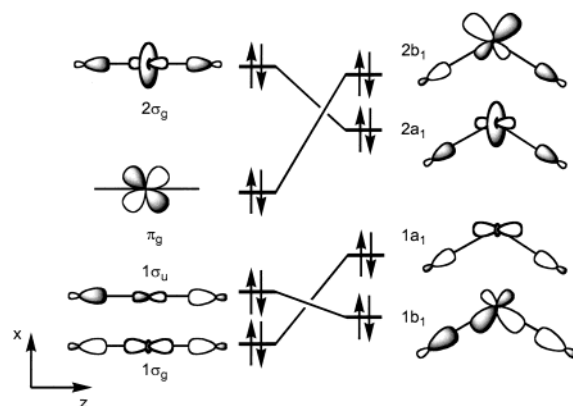(36) Bayler, A.; Schier, A.; Schmidbaur, H. *Inorg. Chem.* **1998**, *37*, 4353.
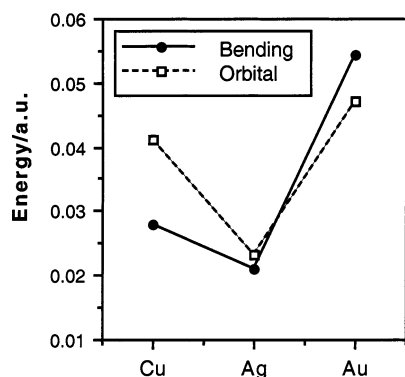
**Figure 11.** Comparison of the energy changes associated to the orbitals depicted in Figure 12 with those in the total energies when an $[M(NH_3)_2]^+$ molecule is bent from 180° to 120°.



**Figure 12.** Schematic behavior of the molecular orbitals that are most affected by bending a linear $[ML_2]^+$ complex to 120°.

characterized compounds of this family have bi-[37] or tridentate phosphines,[20,22] which should be more stable than the model complexes used in our calculations due to the chelate effect. Other members of the family that are known have $MP_3$ fragments that are not fully pyramidalized, as reflected by average X−Au−P bond angles in the range 91−104°, [AgI-$(PPh_3)_3$][38] being probably the only case which is nearly tetrahedral (I−Ag−P bond angle of 106°) and stable, in contradiction with the prediction of our calculations. The softness of the potential energy surface for the association of a fourth ligand that results from the combination of different degrees of interaction and pyramidalization energies is nicely illustrated by two $[AuCl(PR_3)_3]$ complexes: in one of them,[21] the $AuP_3$ fragment is practically planar, with a pyramidality angle of barely 91.3° and the Au−Cl distance is rather long (3.011 Å), whereas, in another one,[39] a larger pyramidalization (99.3°) corresponds to a significantly shorter Au−Cl distance of 2.71 Å.

**Orbital Analysis of the Bending Energy.** Given the important role of the bending energy in determining the lesser tendency of Au to form tricoordinate complexes compared to Cu and Ag, it would be highly interesting to understand the reasons for such a higher bending energy. In that regard, we have analyzed the bending of the $[M(NH_3)_2]^+$ family, for which we have found that the total one-electron energy associated to four occupied molecular orbitals qualitatively reproduces the changes in the bending energy computed from the B3LYP total energy when going down the group (Figure 11). That figure shows that the sum of these orbital energies and the total interaction energy follow the same trend. However, there are quantitative differences that we have found to come from the changes in the two electron terms of the total energy and in the energy of other orbitals. We can understand the larger difference between one-electron and total bending energy for Cu, since electron repulsion terms are much more important (hence more sensitive to changes in delocalization with geometry) for first- than for second- and third-row transition metals.[40]

At the one-electron level, both the $a_1$ and $b_1$ sets of orbitals depicted in Figure 12 significantly contribute to the bending

(37) Affandi, A.; Berners-Price, S. J.; Effendy; Harvey, P. J.; Healy, P. C.; Ruch, B. E.; White, A. H. *J. Chem. Soc., Dalton Trans.* **1997**, 1411.
(38) Camalli, M.; Caruso, F. *Inorg. Chim. Acta* **1987**, *127*, 209.
(39) Jones, P. G.; Sheldrick, G. M.; Muir, J. A.; Muir, M. M.; Pulgar, L. B. *J. Chem. Soc., Dalton Trans.* **1982**, 2123.
(40) Griffith, J. S. *The Theory of Transition-metal Ions*; Cambridge University Press: Cambridge, 1971.

energy. Notice that the diagram presented in Figure 12 is generic for all the three compounds, and the actual orbital energies change from one metal to another. Closer inspection of those orbitals indicates that the differences when going down the periodic group 11 must be attributed to s−d and p−d hybridization (for $a_1$ and $b_1$, respectively) and to the different bond angle dependence of the corresponding overlap integrals. Focusing first on the $a_1$ orbitals, these are in-phase and out-of-phase combinations of the metal $z^2$ with the ligands' lone pair orbitals, showing significant hybridization with the high-lying metal s orbital (notice the different shape of the $z^2$ contribution in $1\sigma_g$ and $2\sigma_g$) that makes the in-phase combination clearly bonding but the out-of-phase combination practically nonbonding. As the molecule is bent, the loss of $z^2$−lone pair overlap affects more $1\sigma_g$ than $2\sigma_g$, resulting in a net destabilization. Since s−d hybridization increases in the order Ag < Cu < Au, so does the destabilization associated with these two orbitals.

Among the $b_1$ orbitals, xz (nonbonding in the linear molecule) overlaps increasingly with the ligands' lone pairs as the molecule is bent and develops antibonding character, whereas the decreased overlap between $p_z$ and the ligands results in the loss of bonding character of $1b_1$ and an overall destabilization. Although p−d mixing reinforces the bonding character of $1b_1$ and decreases the antibonding character of $2b_1$ (Figure 12), still an important net destabilization results, governed by the different angle dependence of the overlap for the three metals, much weaker for Ag than for Cu and Au. As a consequence, the $b_1$ destabilization increases according to Ag < Cu ≈ Au. All in all, the present analysis provides some rationale for the calculated trends that are in agreement with the experimental data. A deeper insight would require a more detailed knowledge of the contribution of two electron terms to the bending energy, and the appropriate tools are currently not available.

## Concluding Remarks

This work was intended to answer three main questions: (1) What determines the coordination number for a given choice of $d^{10}$ metal ion and ligands? (2) Why Au has a much greater tendency for dicoordination compared to Cu and Ag? (3) Why is there a large degree of ambiguity in the assignment of coordination numbers?

(1) To the first question we can now answer that the choice of coordination number is determined by the interplay of two factors: (a) the interaction energy (the more stabilizing it

becomes, the more an increase in coordination number is favored) and (b) the energy required to deform the metal coordination sphere associated to an increase in the coordination number.

(a) As for the influence of the ligands on the interaction energy, phosphines are more stabilizing than ammonia (although there are a few exceptions to this rule), whereas interaction energies with halides follow the sequence Cl > Br > I. Concerning the influence of the metal we can say that interaction energies for Au are in general comparable to those for Cu and Ag, and that interaction of a dicoordinate complex with a phosphine ligand is in general more stabilizing for Cu than for Ag or Au. The study of the solvent effect for tricoordinate Cu shows that complexes predicted to be unstable in the gas phase can be stabilized in solution by using a solvent of the appropriate polarity.

(b) The energy of deformation of the coordination sphere is seen to be much more destabilizing for Au than for Cu and Ag, although fine-tuning of the deformation energy can be obtained by ligand substitution. In general, dicoordinate phosphine complexes are more easily bent than amine analogues, and resistance to bending decreases with halide ligands in the order Cl > Br > I, whereas the energies of pyramidalization of tricoordinate complexes are much less sensitive to the nature of the ligands.[41]

(2) Since the formation energy corresponding to ligand association reactions depend on the interaction and deformation energies and the iteraction energies are seen to be quite similar

for Cu, Ag, and Au with a the same set of ligands, it is the much higher deformation energy required by Au that makes the formation energies less favorable among the tri- and tetracoordinate complexes for Au, compared to the lighter elements, Cu and Ag. The trends in bending and pyramidalization energies down group 11 for all the calculated compounds can be appreciated in two histograms provided as Supporting Information (Figure S5).

(3) While bending a dicoordinate complex (or pyramidalizing a tricoordinate one) requires energy, a larger degree of bending (pyramidalization) results in enhanced interaction energy with an incoming ligand. As a result, the potential energy surfaces for ligand association reactions are quite shallow, and the structure found in a particular case can be at any point along the path from di- to tricoordinate (or from tri- to tetracoordinate) depending on the fine-tuning provided by inductive or steric substituent influence or solvent or crystal packing effects.

**Supporting Information Available:** Details of structural database searches and tables of numerical results: optimized bond distances and angles, formation, interaction, and deformation energies. This material is available free of charge via the Internet at http://pubs.acs.org.

JA038416A

---

(41) Significant differences in the bending energies have been found also among group 12 complexes of the type [M(NH₃)₂]²⁺ (9.1, 8.5, and 12.9 kcal/mol for Zn, Cd, and Hg, respectively), and these differences can be blamed responsible for the distribution of coordination numbers among the divalent ions of these metals, since dicoordination is the most common one for Hg but the less common one for Zn and Cd, according to our structural database searches.